MARS CLIMATE DATABASE v2.0
CRITICAL REVIEW
(ESTEC Contract 11369/95/NL/JG)

S. R. Lewis and P. L. Read

2 March 1999

Abstract

This document is the Critical Review for version 2.0 of the Mars Climate Database (MCD) and replaces *Collins and Lewis* [1997] which discussed version 1.0. A more detailed description of the contents of the MCD is given in *Lewis and Collins* [1999a] and instructions on its usage are given in *Lewis and Collins* [1999b]. This document compares the MCD with such observational data as is available to date and with a previous Mars climate model which has been developed for similar purposes, MarsGRAM [*Justus*, 1990; *Justus et al.*, 1995].

Contents

1 Introduction

The Mars Climate Database (MCD) is a database of statistics which describe the climate and surface environment of Mars and has been based directly on output from multi-annual integrations of two General Circulation Models (GCMs) developed jointly at Laboratoire de Météorologie Dynamique du CNRS, France, and the University of Oxford, U.K., with support from the European Space Agency. The models have been developed and validated to reproduce the main features of the meteorology of Mars, as observed by past spacecraft missions. As well as the more standard statistical measures for mission design studies, the Mars Climate Database includes a novel representation of large scale variability, using empirical eigenfunctions derived from an analysis of the full simulations, and small scale variability using parameterizations of processes such as gravity wave propagation. The database is critically compared here with a representative range of currently available observations and with previous climate models which have been developed for similar purposes, in particular MarsGRAM [*Justus*, 1990; *Justus et al.*, 1995].

A similar critical comparison has already been conducted for version 1.0 of the database [*Collins and Lewis*, 1997]. The present document updates that comparison using data obtained from the MCD version 2.0. For a more detailed description of the MCD and the validation of version 1.0 see *Lewis et al.* [1999]; *Lewis and Collins* [1999a] and *Lewis and Collins* [1999b] describe the structure of the version 2.0 MCD, the details of the dust distribution scenarios and the key differences between version 2.0 and version 1.0. For a description of the GCMs used to compile the MCD, see *Forget et al.* [1999].

One major difference between version 2.0 and 1.0 of the MCD is that the large-scale variability model now makes use of two-dimensional, multivariate Empirical Orthogonal Functions (EOFs), which describe correlations in the model variability as a function of both height and longitude (rather than solely of height as in version 1.0). The evolution of the statistically most significant 72 EOFs for each latitude band are modelled throughout the Mars year. The advantages of this approach, in both increased variance capture and more realistic large-scale variability in both space and time, are described in *Lewis and Collins* [1999a].

A second difference is that two parallel datasets are now included in the climate database distribution. The first has been compiled with the same set of model properties as the version 1.0 database, although the GCMs which were used to compile the database have been extensively validated as a result of the first study and improved in several respects [*Forget et al.*, 1999]. This dataset is referred to as the "standard dust" dataset. A second complete database has also been prepared with an increased dust single scattering albedo in the models [see *Forget et al.*, 1999, for details] and is referred to as the "bright dust" dataset. The "bright dust" properties may give a slightly better fit to a few previous observations of Martian atmospheric temperatures (see Figures 3, 4, 5, 6 and 10) and could be used if only a single dataset is required. The "standard dust" dataset gives a better correspondence with the previous version of the database. Both may be used to check warmer and cooler extremes.

2 Comparison with Observations

This section describes a comparison of previous spacecraft observations of Mars with results predicted at similar locations and times in the MCD. It should be remembered that the MCD has been compiled with temporal averaging and thus the individual observations could not be expected to match the climatology exactly, even if the dust conditions, which are in general poorly known, matched one of the MCD scenarios exactly. The variability models provided with the MCD do allow an ensemble of realizations consistent with climatology to be produced. The extent to which these differ indicates the degree of confidence which may be placed in any one prediction. Comparisons are made with observations of surface pressure, temperature, wind and polar ice caps. Validation against the recent Mars Pathfinder observations are dealt with in a separate section since these permit a validation of the MCD diurnal cycle, in particular, in several variables. Mars Pathfinder provides the first real test of the MCD since the latter was designed and compiled from model runs conducted before these data became available.

2.1 Surface Pressure

During the Viking mission, two landers collected meteorological observations for several Martian years from the northern hemisphere of the planet (Viking lander 1 was situated at 22°N 48°W and Viking lander 2 was situated at 48°N 226°W). Figure 1 shows the Viking 1 and 2 daily averaged surface pressure observations taken from the first Martian year of the mission. The large seasonal cycle is due largely to the condensation and sublimation of CO_2, although there is an important dynamical component [*Hourdin et al.*, 1993], while the high frequency oscillations are due to weather systems passing over the landers [*Barnes*, 1980, 1981; *Collins et al.*, 1996]. Figure 2 shows the MCD Viking dust scenario daily-averaged pressure from the Viking sites. An estimate of the variability due to weather systems, with the seasonal trend component of the MCD variance removed, is also shown. The variance is large in the winter season, in good agreement with the observations, as is the overall shape of the pressure curves. The annual-mean pressure at each site is, however, sensitive to the choice of topographic dataset and of the database resolution. Also shown is the mean pressure from the $\tau = 5$ dust storm scenario at the same time of year as the dust storm seen in Figure 1, confirming that pressures are higher and the variability is somewhat lower at these points under dust storm conditions, consistent with the observations.

2.2 Temperature

Temperature observations from the Martian atmosphere have been obtained from both direct measurements and from a variety of remote sensing measurements from the Earth and from orbiting spacecraft.

Figures 3 and 4 show temperature measurements taken during the entry phases of the Viking landers [*Seiff and Kirk*, 1977] compared with MCD simulations of these profiles. The MCD profiles show both the seasonal mean temperature from the appropriate time in the Viking dust scenario and an example profile which makes use of the small and large scale variability models. The small scale variability is representative of vertically propagating gravity waves, applied with random phase, and is clearly most important at higher altitudes where the observations also

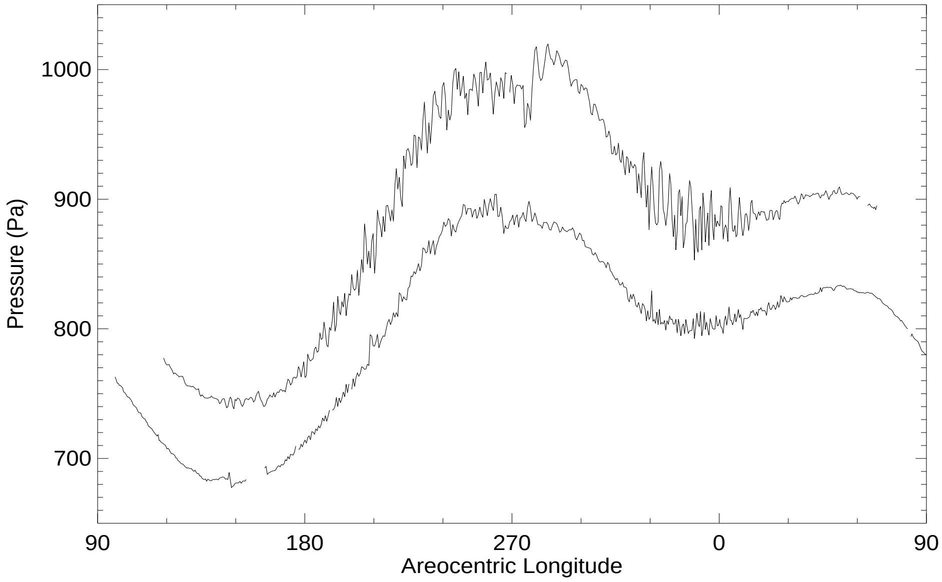

Figure 1: Observed Viking 1 (lower curve) and 2 (upper curve) surface pressure for the first Martian year of observations, averaged to remove the diurnal tide. The high frequency oscillations are caused by weather systems passing over the landers. The jump in pressure, and modulation in the amplitude of the weather signal, close to $L_S = 280°$ was caused by a dust storm. (Data from the Atmospheres Node of the Planetary Data System.)

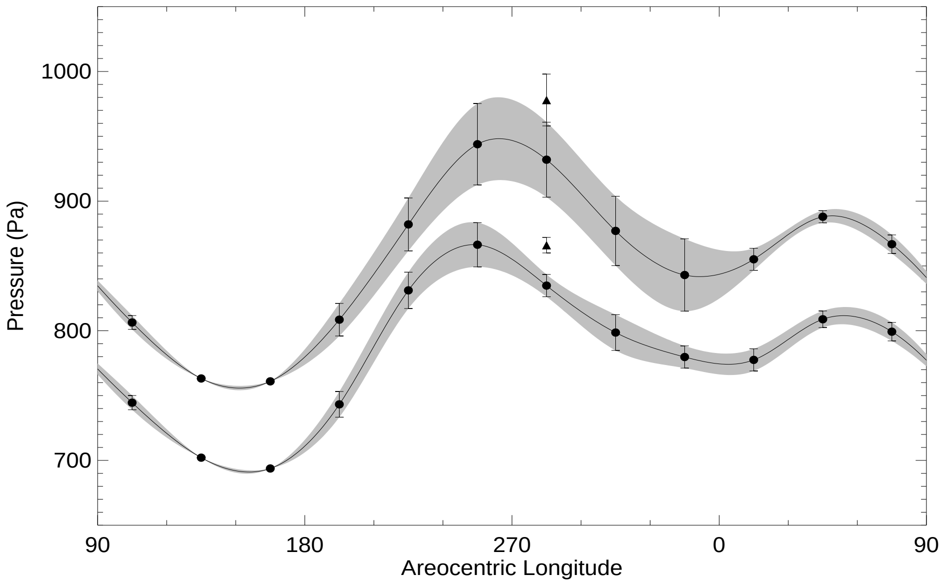

Figure 2: Pressure at the Viking 1 (lower curve) and 2 (upper curve) sites for one year of the MCD Viking dust scenario. The black circles show the diurnally-averaged, seasonal values at intervals of $30° L_S$ and the smooth curve is a cubic spline fit. The error bars and shaded region indicate the non-diurnal variability (2σ) of the surface pressure with the seasonal trend component removed from the total variance. The triangles and error bars at $L_S = 285°$ show the pressure and non-diurnal variance at this time in the $\tau = 5$ dust storm scenario.

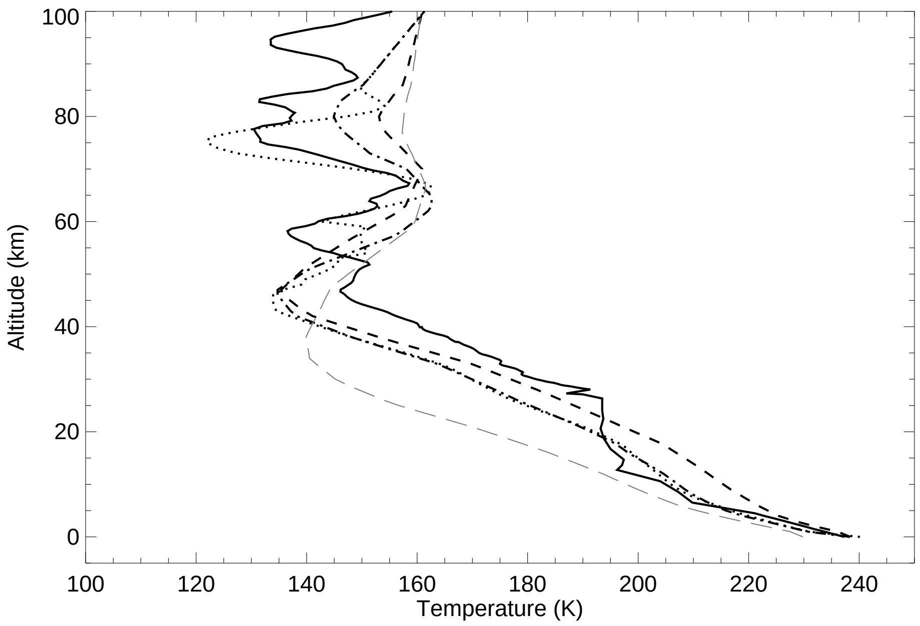

Figure 3: The Viking Lander 1 entry temperature profile (solid), shown with the MCD climatological mean from the Viking dust scenario ("standard dust" line dashed, "bright dust" line dot-dashed), season 4, and one application of the MCD small and large scale variability models to the "bright dust" data (dotted). The grey, long-dashed line shows the low dust scenario mean profile for the same location and time for comparison. The altitude axis shows the height above the local surface. (Viking data provided by A. Seiff and J.R. Murphy.)

seem to indicate wave-like behaviour, though it is not clear to what extent this is due to gravity waves or thermal tides in the observations.

The agreement with the observations appears generally reasonable, although there is some evidence that the MCD "standard dust" data overestimates the temperature by about 10 K in the lower atmosphere, between 5 km and 25 km altitude. The Viking dust scenario may use too simple a specification of the dust distribution; variations in the dust distribution globally or locally might account for the cooler temperatures observed in the lower atmosphere at these locations. The warm bias in both profiles, however, suggests that there might be a bias in the model radiative calculations. The "standard dust" version of the MCD was compiled with model runs which made use of dust single-scattering parameters in the visible based on *Ockert-Bell et al.* [1997]. Since then, the dust single-scattering albedo for the GCMs has been revised, as discussed in detail in *Forget et al.* [1999]. Model integrations with the "bright dust" parameters correct the warm bias noted here in the lower atmosphere. The agreement is better close to the surface and higher in the atmosphere, up to about 80 km altitude at which point non-local thermodynamic equilibrium effects become significant [*Lopez-Valverde and Lopez-Puertas*, 1994]; these are currently only treated simply in the model radiation schemes but an improved treatment to extend the upper limit of the GCMs is planned.

The majority of temperature observations of the Martian atmosphere come from remote sensing of the atmosphere by instruments mounted on orbiting spacecraft. Figures 5 and 6 show a comparison of the MCD low dust and Viking dust scenario temperatures for the appropriate season with the temperatures derived by *Leovy* [1982] from the Mariner 9 IRIS instrument at

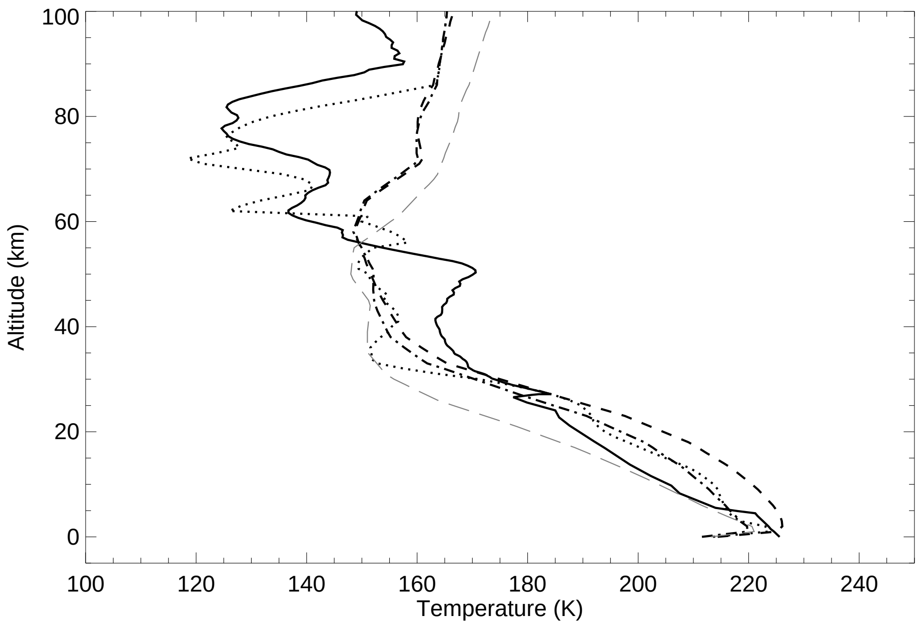

Figure 4: The Viking Lander 2 entry temperature profile (solid), shown with MCD climatologies and variability, labeled as in Figure 3. (Viking data provided by A. Seiff and J.R. Murphy.)

$L_S = 43°$–$54°$. In Figure 5, the IRIS temperatures can be seen to fall between the low dust and Viking dust scenario data, with "standard dust" properties. Figure 6 shows the corresponding data from the "bright dust" dataset; the match between the MCD and the data appears better. Whether this is because of a bias in the "standard dust" properties or because the IRIS data was taken at a time when the atmosphere was cooler and less dusty than the Viking dust scenario is open to question. Hopefully, such uncertainties will be reduced in future with more extensive data from forthcoming spacecraft missions. The different dust scenarios, and choice of dust albedos, within the MCD currently allow a realistic range of possibilities to be considered, from the relatively warm Viking scenario to the colder, low dust scenario and these effectively cover the range of observed temperatures in most cases.

2.3 Wind

Direct observations of winds on Mars are extremely rare [*Zurek et al.*, 1992]. However, winds have been inferred from a variety of secondary effects, such as streak features on the Martian surface [*Thomas et al.*, 1984]. These observations suffer from problems of incomplete global coverage and uncertainties in exactly how and when the features were formed, but have previously been used as a basis for a comparison with the Ames Mars GCM [*Greeley et al.*, 1993]. Figure 7 shows a set of wind directions inferred from wind streak data [*Magalhães*, 1987]; these can be compared with low level winds from the MCD, shown in Figure 8, for the period $L_s = 270°$–$300°$ corresponding to the approximate time at which the streaks might have formed and under medium, $\tau = 2$, dust storm conditions, since the streaks are thought to have formed during the decay phase of a global dust storm. Although there are considerable uncertainties in the appropriate dust loading, range of times to average over and heights at which to sample the winds, Figures 7 and 8 do show strong similarities. In particular, both zonally-averaged diagrams show evidence of predominant westerlies at high northern latitudes, a region of north-easterlies north

(a) Temperature (K) observed by Mariner 9 IRIS (L_s =43°–54°)

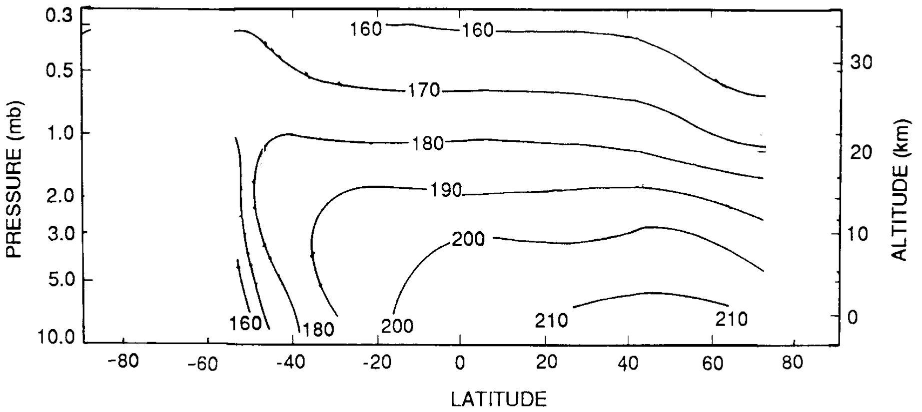

(b) Temperature (K) from the MCD low dust scenario

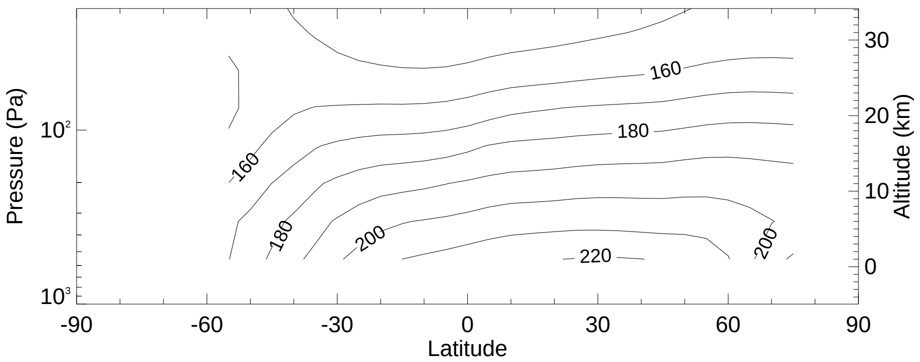

(c) Temperature (K) from the MCD Viking dust scenario

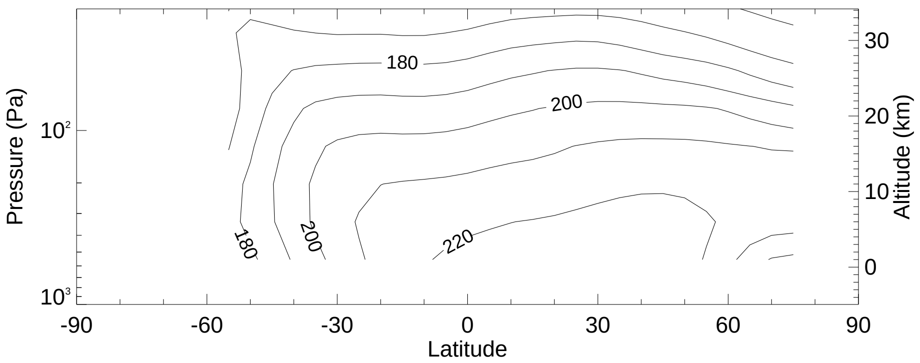

Figure 5: The thermal structure observed by the IRIS instrument aboard Mariner 9 in 1972 [*Leovy*, 1982] during northern spring (L_s =43°–54°), compared to the zonally averaged temperatures from the MCD using the "standard dust" dataset.

(a) Temperature (K) observed by Mariner 9 IRIS (L_s =43°–54°)

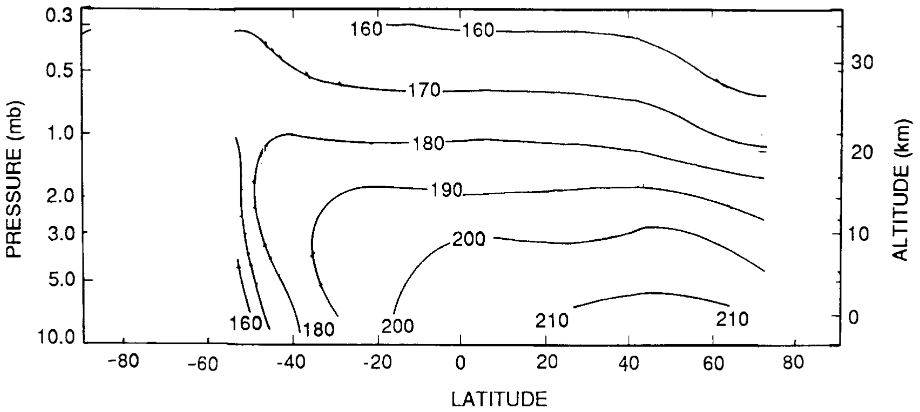

(b) Temperature (K) from the MCD low dust scenario

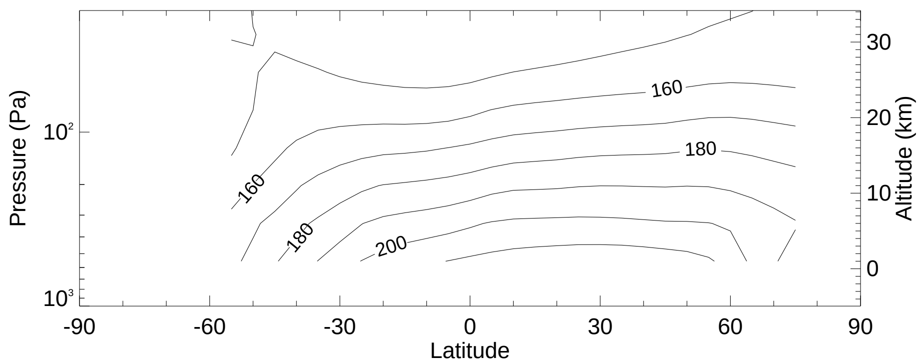

(c) Temperature (K) from the MCD Viking dust scenario

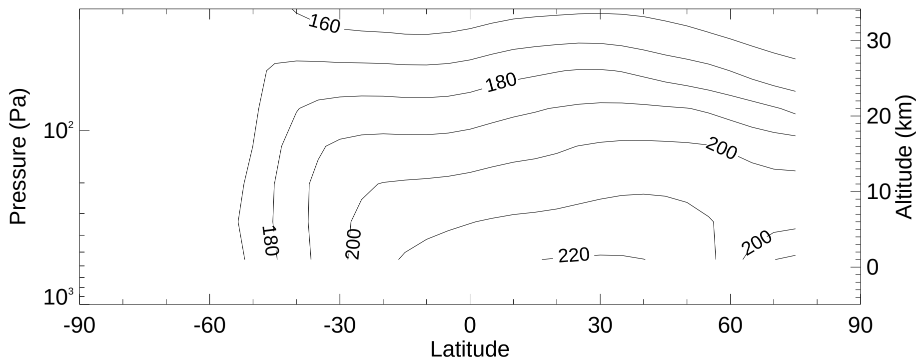

Figure 6: The thermal structure observed by the IRIS instrument aboard Mariner 9 in 1972 [*Leovy*, 1982] during northern spring (L_s =43°–54°), compared to the zonally averaged temperatures from the MCD using the "bright dust" dataset.

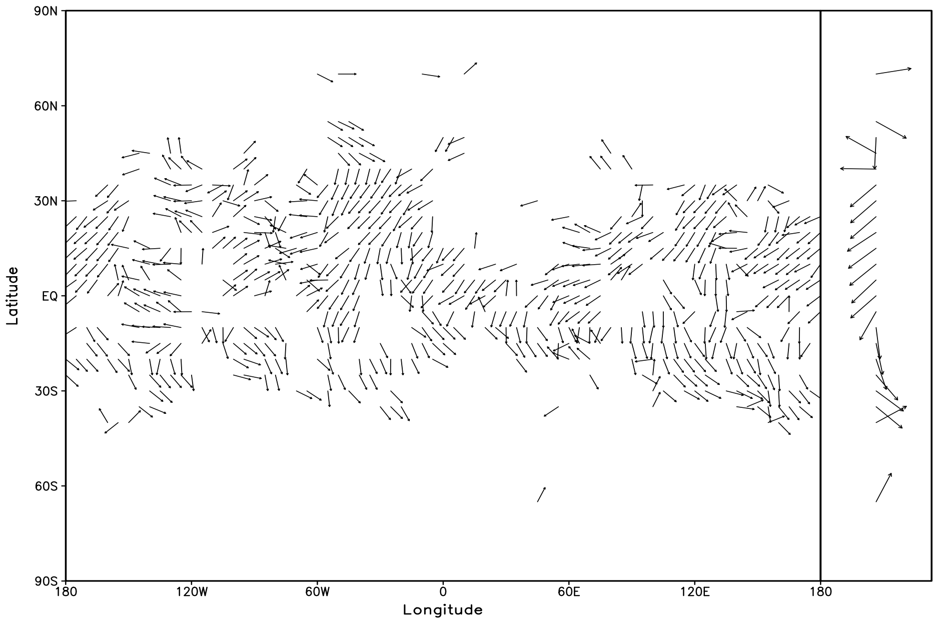

Figure 7: Distribution of "Type I(b)" surface streak orientations derived from Viking Orbiter mosaics. The "Type I(b)" streaks are thought to indicate the directions of near-surface winds during the decay of the global dust storms in 1977. Average azimuths are shown for for $5° \times 5°$bins. The right panel shows the zonal average of the binned streak directions; note that there are relatively few observations more than about 30° latitude from the equator. (Average direction data provided by J.A. Magalhães [*Magalhães*, 1987], using data from P.C. Thomas [*Thomas et al.*, 1984].)

of the equator with rotation back to north-westerlies in the southern midlatitudes. This pattern in the subtropics is consistent with a single, cross-equatorial cell in the mean meridional circulation [*Magalhães*, 1987]. There are also similarities in the MCD wind and observed streak directions in the longitude–latitude maps in several regions where there are observations. For example, there are coherent regions of northerly, cross-equatorial flow near 50°W in both figures, consistent with a western boundary current at the edge of the Tharsis ridge [*Joshi et al.*, 1995]. Difficulties in the interpretation of the streak data make a strict comparison impossible, but we conclude that the database winds appear generally consistent with the observations.

2.4 Polar Caps

Figure 9 shows the time-mean equivalent latitudes for the edges of the polar caps of carbon dioxide ice for the four scenarios from the MCD. The equivalent latitude is that which would be reached by a perfectly symmetrical cap occupying the same area as the total area of ice coverage in that hemisphere. Also shown are actual observations of the edges of the Martian ice caps for comparison. The agreement appears good, indicating that the climatological surface temperature, and hence conditions for CO_2 ice formation and sublimation, are well predicted by the MCD models. There is perhaps some evidence of a small overestimation of the extent of the caps in the MCD. Two effects may partly contribute to this. The procedure for determining the effective size of the caps in the MCD involved adding the areas of all grid boxes in which

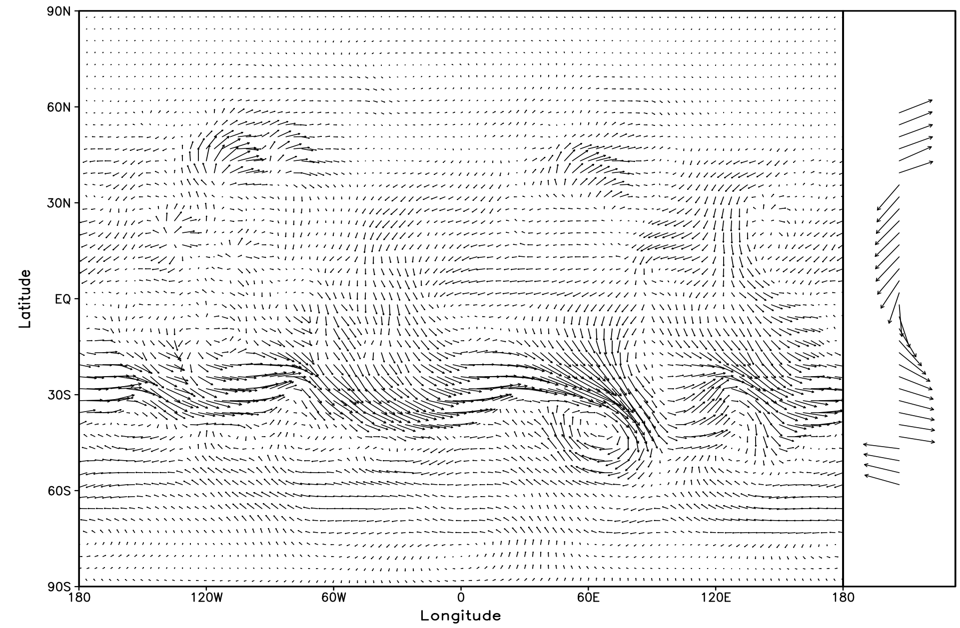

Figure 8: Winds taken from the lowest level of the MCD and diurnally-averaged over season 10 ($L_s = 270°$– $300°$) of the $\tau = 2$ dust storm scenario. The right panel shows the zonal-mean wind direction between 60°S and 60°N, to be compared with Figure 7.

any ice was present at all, tending to result in an overestimate if boxes should only be partially icy. It is also not clear what thickness of ice cover is required to be present before the presence of a polar cap is detected in the observations.

2.5 Prediction of Mars Pathfinder Observations

The Atmospheric Structure Investigation/Meteorology experiment [*Schofield et al.*, 1997] on the Mars Pathfinder spacecraft provided the first independent test of the MCD, since the database was compiled from simulations designed before observations from the mission became available. These new observations are compared with the MCD in this section.

The entry temperature profile retrieved for Mars Pathfinder [*Magalhães et al.*, 1999] was compared with the MCD, shown in Figure 10. As with the Viking Lander entry profiles (Figures 3 and 4), the observations fall close to the Viking dust climatology from the "bright dust" dataset. The thermal inversion observed near 15 km altitude is presumed to be due to an ice cloud [*Schofield et al.*, 1997], which is not represented in the GCMs, and here the MCD is much warmer. The MCD produced a profile similar to those for the Viking Lander 1 profile (Figure 3), except that the variability model predicted a slightly larger degree of small scale variability in the upper atmosphere at the Pathfinder site, reflecting enhanced wave activity because of higher near-surface wind speeds. This allowed temperatures as low as 80 K to be reached in some cases, as observed in the temperature retrieval.

The Mars Pathfinder observations of surface pressure, temperature and wind direction over the primary thirty day phase of the mission [*Schofield et al.*, 1997] allow the MCD representation of the diurnal cycle to be tested in some detail. Both the observations and the MCD indicate very little non-diurnal variability, other than the seasonal trend, at the Pathfinder site at the

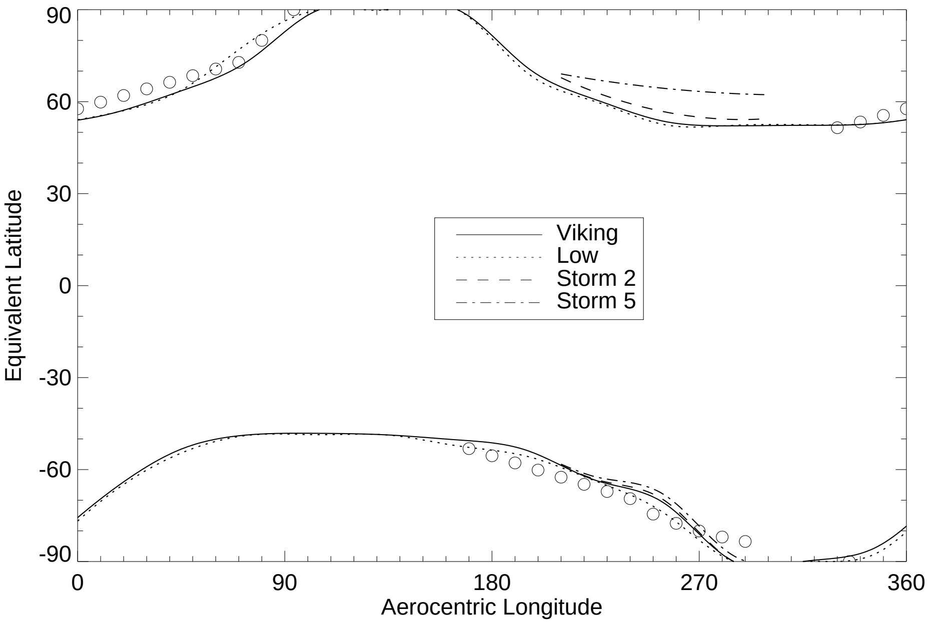

Figure 9: Mean equivalent latitudes for the edges of the polar caps of carbon dioxide ice for the four scenarios from the MCD, labeled according to the usual convention. The circles indicate actual observations of the edges of the Martian caps (data provided by J.B. Pollack).

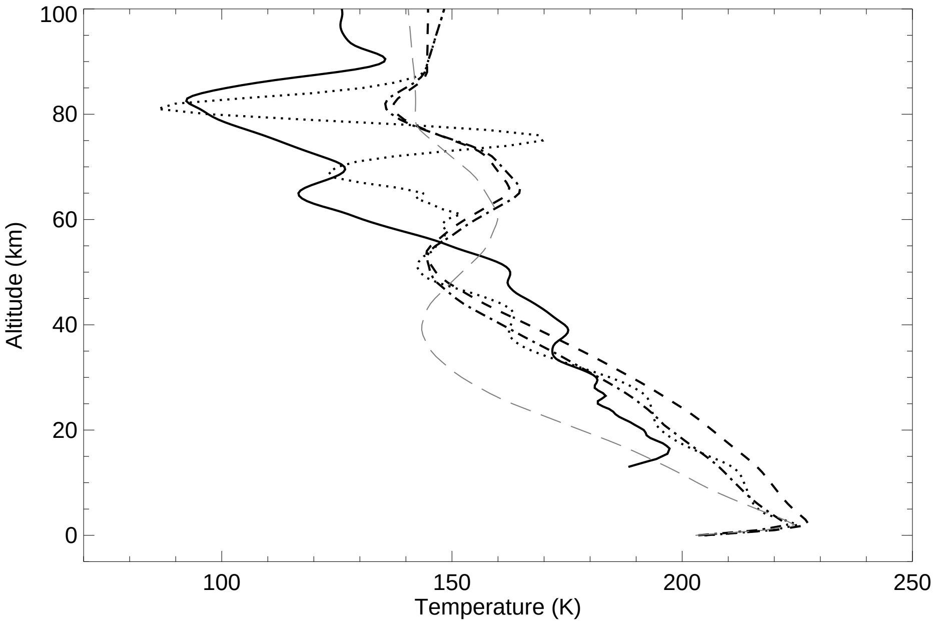

Figure 10: The Mars Pathfinder entry temperature profile (solid), shown with MCD climatologies and variability, labeled as in Figure 3. (Pathfinder data provided by J.A. Magalhães [*Magalhães et al.*, 1999].)

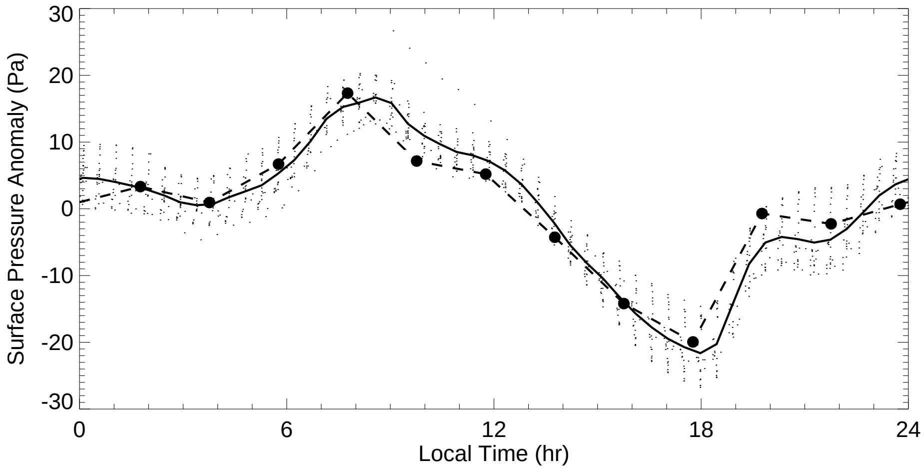

Figure 11: A comparison of the Mars Pathfinder surface pressure diurnal cycle with the MCD. The small dots show the Mars Pathfinder pressure measurements, taken about 51 times per day, and the solid line is the mean of the observations taken over the first 30 days of the mission. The large circles connected by dashed lines show the MCD mean surface pressure at the Mars Pathfinder location. In both cases the diurnal-mean surface pressure has been subtracted; 666 Pa in the case of the Pathfinder data and 686 Pa in the case of the MCD.

	Amplitude (Pa)		Phase (hr)	
Period	MPF	MCD	MPF	MCD
Diurnal	11.9	10.7	6.6	6.1
Semi-Diurnal	6.9	6.1	10.4	9.7

Table 1: Surface Pressure Tides at the Pathfinder site. Mars Pathfinder observations are labeled MPF, database results are labeled MCD. Phase is given as the local time of first maximum.

time of year at which the mission landed ($L_S = 142°$); however, the diurnal cycle is strong.

The seasonal mean surface pressure cycle is compared with Pathfinder data in Figure 11 and can be seen to be in excellent agreement with the observations. The amplitudes and phases of the diurnal and semi-diurnal tides were also calculated both from the observations and from the MCD and show good agreement in both cases; see Table 1. Figure 12 shows the temperature on the Pathfinder meteorological mast compared with MCD predictions, and Figure 13 shows the wind direction; unfortunately, the wind amplitude is not well calibrated in the observations at this stage and cannot be compared. In each case the MCD prediction is remarkably good, especially considering the spatial resolution of the database and the comparison with a single point observation. It is therefore possible to have confidence in the representation of the diurnal cycle in the MCD, at least in as far as it is possible to test it at this stage.

3 Comparison with MarsGRAM v3.5

In planning previous missions to Mars, environmental statistics have been collected and summarized in the Mars Global Reference Atmosphere Model, MarsGRAM [*Justus*, 1990; *Justus et al.*,

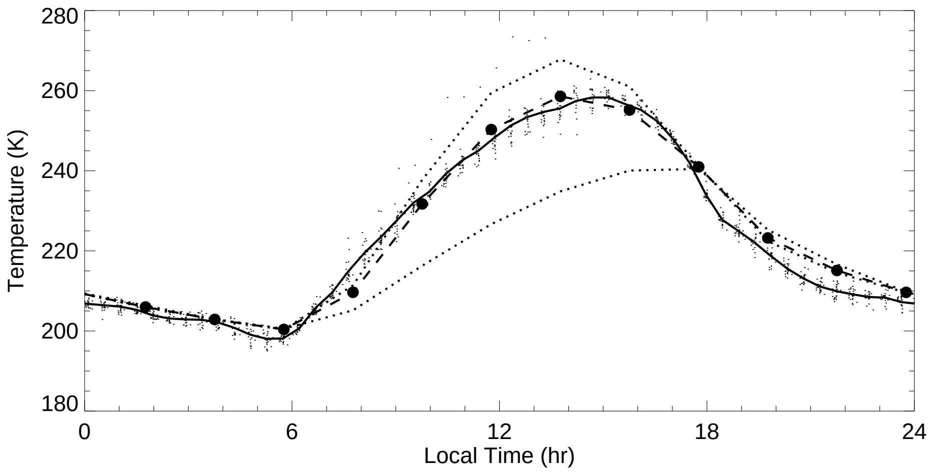

Figure 12: A comparison of the Mars Pathfinder temperature at the top of the 1 m meteorological mast with the MCD. As in Figure 11, the small dots show the individual measurements and the solid line is the mean over 30 days. The dotted lines are the MCD surface temperature (upper line at midday) and the MCD lowest atmospheric level temperature (lower line) which is at a height of about 5 m. The large circles connected by dashed lines show a linear interpolate between the two at a height of about 1.4 m, corresponding to the top of the Pathfinder mast for comparison.

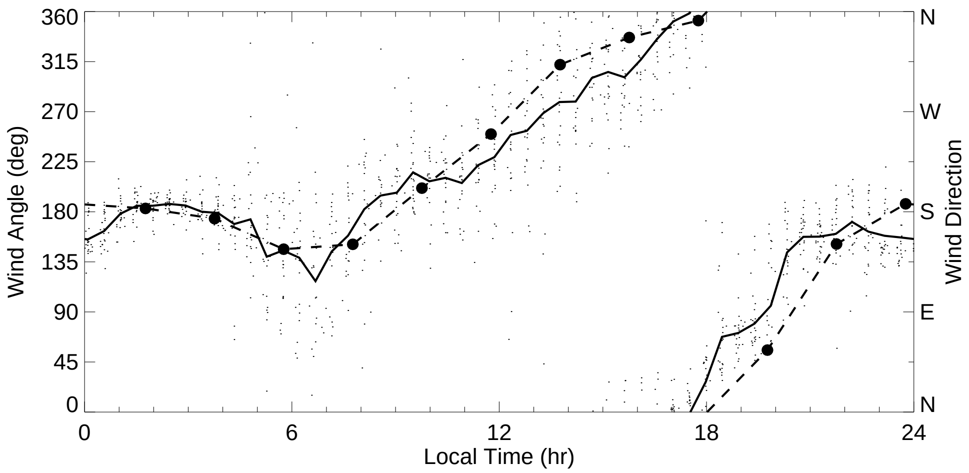

Figure 13: A comparison of the Mars Pathfinder wind direction with that at the lowest atmospheric layer in the MCD. As in Figure 11, the small dots show the individual measurements and the solid line is the mean over 30 days. The large circles connected by dashed lines show the mean wind direction from the same point in the MCD. The wind direction axis indicates the compass point which the wind is blowing from, a wind angle of 0°is a northerly. The general sense of rotation is determined by the passage of the diurnal thermal tide, the details, such as the small rotation towards an easterly near dawn before the subsequent rotation to a westerly, are a consequence of the details of the topography.

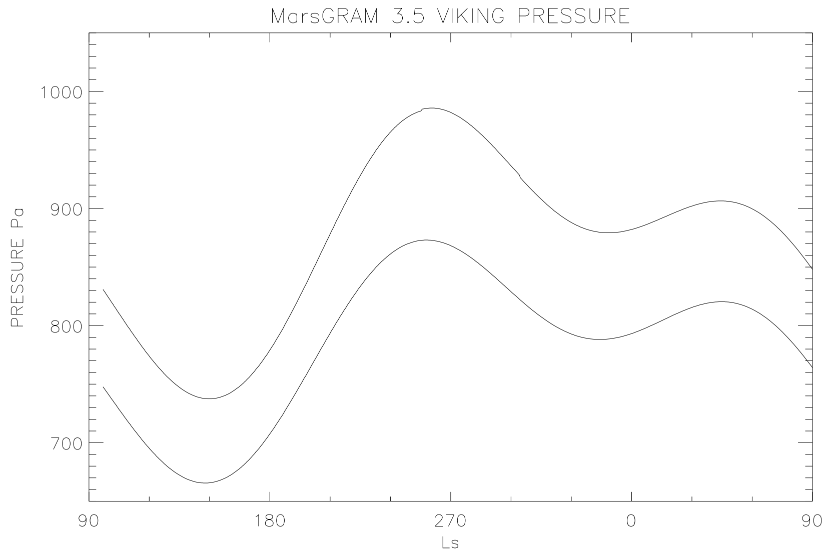

Figure 14: MarsGRAM Viking 1 (lower curve) and 2 (upper curve) surface pressure for one Martian year.

1995]. MarsGRAM uses a blend of observational data and simple physical models to produce realizations of environmental conditions. For example, temperatures are generated by fitting a series of arbitrary functions to the Mariner 9 and Viking thermal measurements, and winds are derived from this using thermal wind balance. While MarsGRAM may produce reasonable fields of observable variables like surface pressure and temperature at seasons and dust loadings where observations exist, ultimately its accuracy is limited by errors in the interpolation between sparse data and on the assumptions used in the physical formulae used to derive the unobserved variables. For example, thermal wind balance is only a good approximation in the middle to high latitudes.

In this section the Mars Climate Database is compared with MarsGRAM version 3.5.

3.1 Surface Pressure

Figure 14 shows the MarsGRAM v3.5 surface pressure from the Viking lander locations for one year. The agreement with the observed pressure (Figure 1) is very good as MarsGRAM fits a functional form to the observed seasonal pressure. However MarsGRAM provides no information on the synoptic variability whereas the MCD does. Also it must be noted that not all the seasonal cycle in pressure is due to the condensation-sublimation cycle. There can be a significant component due to density gradients within the atmosphere [*Hourdin et al.*, 1993]. This phenomenon is clear when looking at seasonal pressure curves from other points on the planet. Figure 15 shows the daily averaged pressure taken from a point within the Hellas basin (longitude 300°W, latitude 40°S) from the MCD and Figure 16 shows the pressure taken from MarsGRAM. There is a marked difference in the seasonal pressure cycle compared to the pressure cycles at the Viking sites due to the dynamical component. This is one of the key advantages of using the MCD rather than fitting seasonal pressure curves to the observed Viking data at two locations.

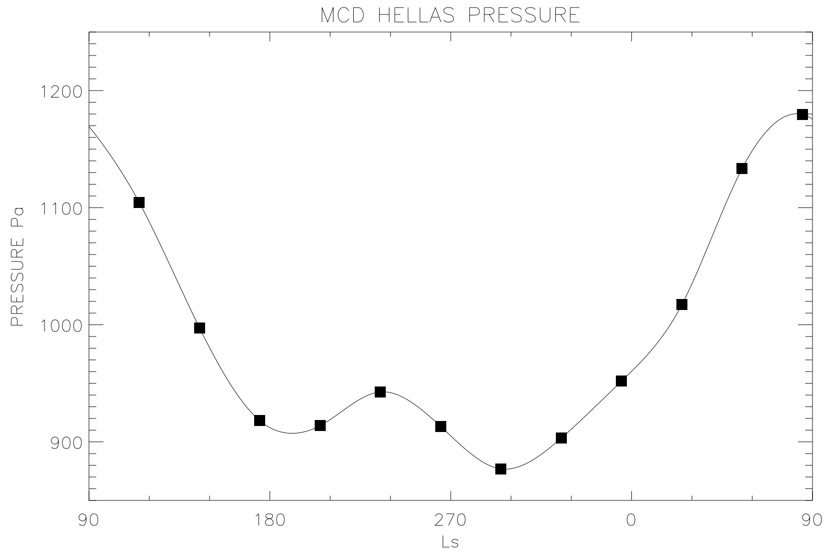

Figure 15: MCD surface pressure for one Martian year at longitude 300°W, latitude 40°S, i.e. the Hellas basin. The black squares show the MCD diurnally averaged seasonal values and intervals of 30°L_s and the smooth curve is a cubic spline fit to these values.

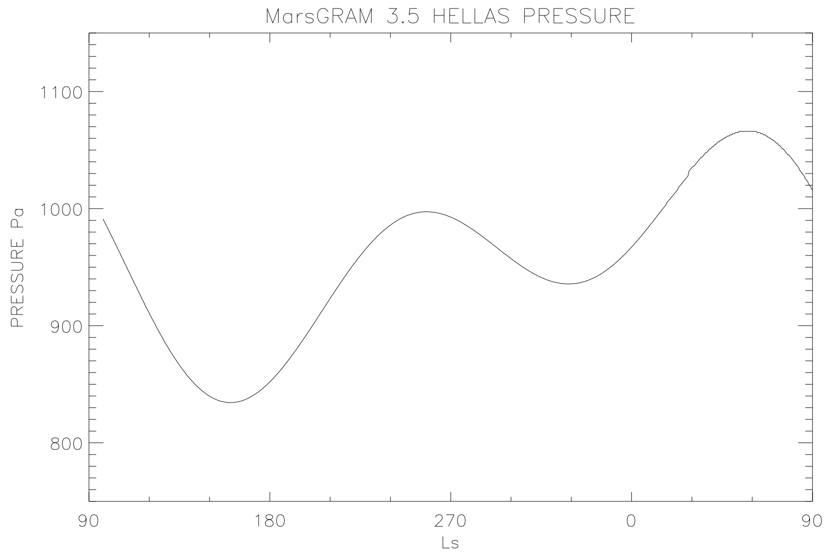

Figure 16: MarsGRAM surface pressure for one Martian year at longitude 300°W, latitude 40°S, i.e. the Hellas basin. To be compared with Figure 15.

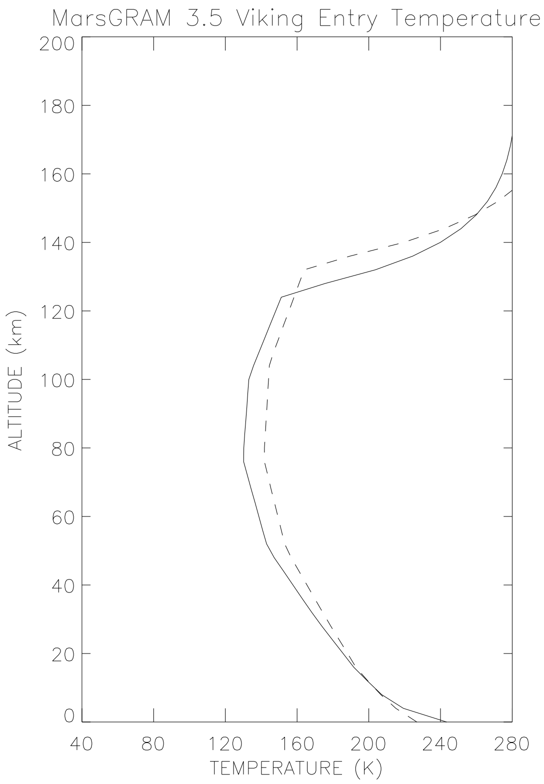

Figure 17: MarsGRAM Viking 1 (solid) and Viking 2 (dashed) entry temperature profiles.

3.2 Temperature

Figure 17 shows the MarsGRAM v3.5 simulated Viking entry temperature profiles to be compared with the observations and the MCD profiles shown in FigureS 3 and 4. As with the surface pressure data at the Viking sites, MarsGRAM is in good agreement with the mean profile but does not have a representation of variability. Although it is possible to add red noise to the MarsGRAM profiles this does not necessarily give a realistic representation of the correlation and cross-correlation scales between different variables.

The comparison of MarsGRAM v3.5 and the Mariner 9 IRIS temperatures from *Leovy* [1982] is shown in Figure 18. The comparison is very good, especially at upper levels where MarsGRAM captures the cold temperatures at this less dusty season. The agreement is less good towards the north polar regions where MarsGRAM predicts a strong horizontal gradient in temperature. However, the overall good agreement is due to the fact that MarsGRAM temperatures are partially derived from a fit to these observations. The MCD has not been optimized in such a way; the dust distributions, which to a large extent determine the vertical temperature gradient, have been chosen to represent a wide range of possible conditions on Mars, not the specific conditions at the time of these observations.

(a) Temperature (K) observed by Mariner 9 IRIS (L_s =43°–54°)

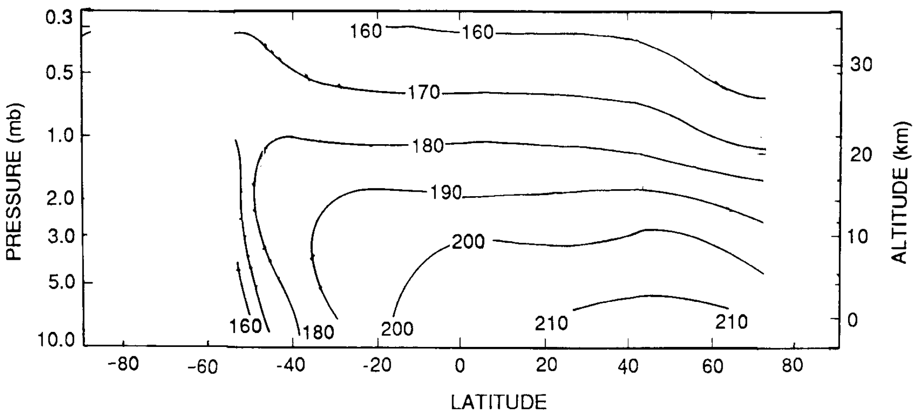

(b) Temperature (K) from MarsGRAM

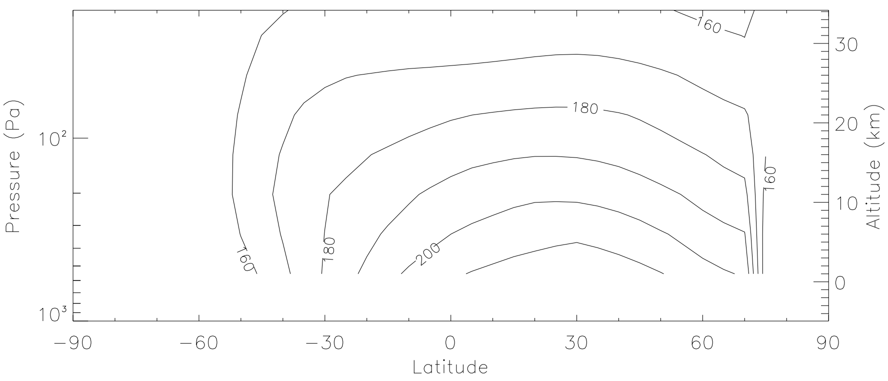

Figure 18: The thermal structure observed by the IRIS instrument aboard Mariner 9 in 1972 [*Leovy*, 1982] during northern spring (L_s =43°–54°), compared to the zonally averaged temperatures from MarsGRAM.

4 Conclusions

This document is a comparison of the Mars Climate Database version 2.0 with observational data and with MarsGRAM, the most commonly used engineering model of Mars. The MCD has been compiled from the results of GCM experiments, rather than directly from empirical fits to observational data. The Mars GCM parameters used to compile the MCD have been taken where possible to be consistent with independent estimates of these parameters, and to obtain model results which are consistent with most of the the available observational data for the atmosphere of Mars, obtained primarily by the Mariner 9 and Viking spacecraft. However, such observations are sparse in both spatial and temporal coverage. One particular strength of using a GCM to compile such a database, in contrast to MarsGRAM, is that it provides a physically consistent estimate of the environmental conditions on Mars for locations, seasons and dust loadings which are not covered by the observations. MarsGRAM predicts conditions for these regions based upon simple interpolation procedures, which have been demonstrated to be inaccurate, and could even be misleading in some cases. The MCD is also able to model both large- and small-scale variability in a plausible way using models described in *Lewis and Collins* [1999a]. The MCD has been validated against observations, including the latest ones from the Mars Pathfinder mission, and is found to produce broadly realistic results.

References

Barnes, J. R., Time spectral analysis of mid-latitude disturbances in the martian atmosphere, *J. Atmos. Sci.*, *37*, 2002–2015, 1980.

Barnes, J. R., Midlatitude disturbances in the martian atmosphere: A second Mars year, *J. Atmos. Sci.*, *38*, 225–234, 1981.

Collins, M., and S. R. Lewis, Mars Climate Database v1.0: Critical review, *Tech. rep.*, European Space Agency Technical Report, 1997.

Collins, M., S. R. Lewis, P. L. Read, and F. Hourdin, Baroclinic wave transitions in the martian atmosphere, *Icarus*, *120*, 344–357, 1996.

Forget, F., F. Hourdin, R. Fournier, C. Hourdin, O. Talagrand, M. Collins, S. R. Lewis, P. L. Read, and J.-P. Huot, Improved general circulation models of the martian atmosphere from the surface to above 80 km, *J. Geophys. Res.*, 1999, in press.

Greeley, R., A. Skypeck, and J. B. Pollack, Martian aeolian features and deposits: Comparisons with general circulation model results, *J. Geophys. Res.*, *98*, 3093–3123, 1993.

Hourdin, F., P. Le Van, F. Forget, and O. Talagrand, Meteorological variability and the annual surface pressure cycle on Mars, *J. Atmos. Sci.*, *50*, 3625–3640, 1993.

Joshi, M. M., S. R. Lewis, P. L. Read, and D. C. Catling, Western boundary currents in the martian atmosphere: Numerical simulations and observational evidence, *J. Geophys. Res.*, *100*, 5485–5500, 1995.

Justus, C. G., A Mars Global Reference Atmosphere Model (Mars-GRAM) for mission planning and analysis, in *AIAA 28th Aerospace Sciences Meeting*, 1990, paper No. 90–0004.

Justus, C. G., F. N. Alyea, D. M. Cunnold, W. R. Jeffries III, and D. L. Johnson, The NASA/MSFC Global Reference Atmosphere Model – 1995 version (GRAM-95), *Tech. rep.*, NASA, 1995.

Leovy, C. B., Martian meteorological variability, *Adv. Space Res.*, *2*, 19–44, 1982.

Lewis, S. R., and M. Collins, Mars Climate Database v2.0: Detailed design document, *Tech. rep.*, European Space Agency Technical Report, 1999a.

Lewis, S. R., and M. Collins, Mars Climate Database v2.0: User manual, *Tech. rep.*, European Space Agency Technical Report, 1999b.

Lewis, S. R., M. Collins, P. L. Read, F. Forget, F. Hourdin, R. Fournier, C. Hourdin, O. Talagrand, and J.-P. Huot, A Climate Database for Mars, *J. Geophys. Res.*, 1999, in press.

Lopez-Valverde, M. A., and M. Lopez-Puertas, A non-local thermodynamic equilibrium radiative transfer model for infrared emissions in the atmosphere of Mars 1. theoretical basis and nighttime populations of vibrational states, *J. Geophys. Res.*, *99*, 13,093–13,115, 1994.

Magalhães, J. A., The martian Hadley circulation: Comparison of "viscous" model predictions to observations, *Icarus*, *70*, 442–468, 1987.

Magalhães, J. A., J. T. Schofield, and A. Seiff, Results of the Mars Pathfinder Atmospheric Structure Investigation, *J. Geophys. Res.*, 1999, in press.

Ockert-Bell, M. E., J. F. B. III, C. McKay, J. Pollack, and F. Forget, Absorption and scattering properties of the martian dust in the solar wavelengths, *J. Geophys. Res.*, *102*, 9039–9050, 1997.

Schofield, J. T., D. Crisp, J. R. Barnes, R. M. Haberle, J. A. M. aes, J. R. Murphy, A. Seiff, S. Larsen, and G. Wilson, The Mars Pathfinder Atmospheric Structure Investigation/ Meteorology (ASI/MET) experiment, *Science*, *278*, 1752–1757, 1997.

Seiff, A., and D. B. Kirk, Structure of the atmosphere of Mars in summer at mid-latitudes, *J. Geophys. Res.*, *82*, 4364–4378, 1977.

Thomas, P. C., J. Veverka, D. Gineris, and L. Wong, "dust" streaks on Mars, *Icarus*, *49*, 398–415, 1984.

Zurek, R. W., J. R. Barnes, R. M. Haberle, J. B. Pollack, J. E. Tillman, and C. B. Leovy, Dynamics of the atmosphere of Mars, in *Mars*, edited by H. H. Kieffer, B. M. Jakosky, C. W. Snyder, and M. S. Matthews, pp. 835–933, University of Arizona Press, Tucson, 1992.